Accepted Manuscript

Guest: Host interactions of lidocaine and prilocaine with natural cyclodextrins: Spectral and molecular modeling studies

N. Rajendiran, T. Mohandoss, J. Saravanan

PII: S1386-1425(14)00696-9
DOI: http://dx.doi.org/10.1016/j.saa.2014.04.123
Reference: SAA 12087

To appear in: *Spectrochimica Acta Part A: Molecular and Biomolecular Spectroscopy*

Received Date: 5 March 2014
Revised Date: 9 April 2014
Accepted Date: 22 April 2014

Please cite this article as: N. Rajendiran, T. Mohandoss, J. Saravanan, Guest: Host interactions of lidocaine and prilocaine with natural cyclodextrins: Spectral and molecular modeling studies, *Spectrochimica Acta Part A: Molecular and Biomolecular Spectroscopy* (2014), doi: http://dx.doi.org/10.1016/j.saa.2014.04.123

Guest: Host interactions of lidocaine and prilocaine with natural cyclodextrins: Spectral and molecular modeling studies

N. Rajendiran*, T.Mohandoss, J.Saravanan

Department of Chemistry, Annamalai University, Annamalai nagar - 608 002, Tamil Nadu, India

*Corresponding author Email: drrajendiran@rediffmail.com

Mobile: +91 94866 28800

Abstract

Inclusion complex formation of two local anesthetics drugs (lidocaine (LC) and prilocaine (PC)) with α- and β-cyclodextrins (CDs) in aqueous solution were studied by absorption, fluorescence, time-resolved fluorescence and molecular modeling methods. The formation of inclusion complexes was confirmed by ^{1}H NMR, FTIR, differential scanning calorimetry, SEM, TEM and X-ray diffractometry. Both drugs formed 1:1 inclusion complex and exhibit biexponential decay in water whereas triexponential decay in the CD solution. Nano sized self-aggregated particles of drug: CD complexes were found by TEM. Both experimental and theoretical studies revealed that the phenyl ring with the amide group of the drug is encapsulated in the hydrophobic CD nanocavity. Investigations of energetic and thermodynamic properties confirmed the stability of the inclusion complexes. van der Waals interactions are mainly responsible for enthalpy driven complex formation of LC and PC with CDs.

Keywords lidocaine, prilocaine, cyclodextrin, inclusion complex, nanoparticles, molecular modeling

1. Introduction

Cyclodextrins (CDs) are cyclic oligosaccharides composed of α-1,4-glycoside linkages, the most common members of this family are α-, β- and γ-CD, which are made up of six, seven and eight D-glucose units [1-4]. By shape, the CDs are torus, having an inner hydrophobic cavity and the outer hydrophilic surface consisting of primary and secondary hydroxyl group edges. The most remarkable property of the CDs is their ability to form inclusion complexes with a variety of organic guest molecules [5-7]. Many hydrophobic guests of appropriate shape and size are known to form supramolecular host-guest complexes with specific CDs and can solubilized in aqueous and solid state. This unique property of the CDs has led to widespread applications in pharmaceuticals, food technology, chemical industries and many other applied areas [8].

In the last few decades a number of spectroscopic techniques have been used to understand the nature of the interaction of CDs with various guest molecules. Fluorescence spectroscopy has been found to be an excellent technique for characterizing the binding of organic molecules in the CD cavities. Other techniques such as absorption spectroscopy, circular dichroism, fluorescence lifetime, electrochemical methods, infra red, powder X-ray diffraction and NMR spectroscopy have been used comprehensively to understand the nature of the host-guest interactions [9,10]. The presence of the hydrophobic environment inside the CD cavity and the restricted movement of the guest molecule inside these cavities controlled the photophysical and photochemical properties of the latter. In recent years, many investigators have employed such properties of the CD inclusion complexes to understand the mechanistic details of many processes such as isomerization reactions, twisted intramolecular charge transfer (TICT) process, etc [11-15].

Recently, we have studied many molecules where the proton donor groups are $–NH_2$, $-OCH_3$ and -OH but the proton acceptor groups are N=N, =N-, C=O, etc [11-22]. Our earlier studies suggested that the specific hydrogen bonding between the solvents/ cyclodextrins and

carbonyl group plays a major role in the formation of the ICT state in the ground state. We reported the polarity of the medium, the specific interactions of the solvent molecules with electron donor and acceptor group can facilitate the formation of the ICT state. In continuation of our work, in this paper we have studied two local anesthetics drugs (lidocaine (2-(diethylamino)- N-(2,6-dimethylphenyl) acetamide) and prilocaine ((RS)-N-(2-methylphenyl)-N^2-propylalaninamide), Fig 1) with α-CD and β-CD. The main aims of the present study are: (i) to compare the effect of the electron withdrawing drug molecules on the ICT emission and (ii) the inclusion complexes whether increase or decrease the longer wavelength (LW) emission. In this paper, we applied absorption and fluorescence spectral techniques to determine the stoichiometry and binding constant of drug: CD inclusion complexes and characterize the inclusion complexes by time-resolved fluorescence spectra, FTIR, ^{1}H NMR, differential scanning calorimetry (DSC), scanning electron microscopy (SEM), transmission electron microscopy (TEM) and powder X-ray diffraction (XRD). Semiempirical quantum mechanical calculations (using PM3 method) propose the geometrical configuration of the inclusion complexes.

2. Material and methods

2.1. Materials

Lidocaine (LC), prilocaine (PC), α-CD and β-CD were purchased from Sigma-Aldrich chemical company and used as such. All other chemicals and solvents used were of the highest grade (Spectrograde) commercially available. Triply distilled water was used for the preparation of aqueous solutions. The aqueous solutions were prepared just before each measurement. Purity of the compounds was checked by melting point and also by using fluorescence techniques i.e., by getting same spectral profile when excited with different wavelengths.

2.2. Preparation of inclusion complexes in solution

A stock solution of drug was prepared in methanol and the concentration of stock solution of the drug was 2×10^{-3} mol dm^{-3}. Exactly 0.2 mL of this stock solution was transferred into each

of the 10 ml volumetric flasks. To this, varying concentrations of α-CD or β-CD solution (1.0×10^{-3} to 1.2×10^{-2} mol dm^{-3}) was added. The mixed solution was diluted to 10 Ml with triply distilled water, shaken thoroughly and kept for 6 hrs to bring it to a state of equilibrium. The final concentration of the drug in all the flasks was 4×10^{-5} mol dm^{-3}.

2.3. Preparation of solid inclusion complexes

α-CD/ β-CD (0.973/1.14 g) was dissolved in 40 ml distilled water at 50 °C in a water bath. The drug (0.234 g for LC or 0.256 g for PC) in 10 ml methanol was slowly added to the CD solution with continuous agitation. The molar ratio of drug to CD was 1:1. The vessel was covered with aluminium foil and stirred continuously for 24 hrs at room temperature and the solution was refrigerated overnight at 5 °C. The precipitated drug: α-CD and drug: β-CD complexes were recovered by filtration and washed with small amount of methanol and water to remove uncomplexed drug and CD respectively. The precipitate was then dried in vacuum at room temperature for two days and stored in an airtight bottle.

2.4. Instruments

Absorption and fluorescence spectral measurements were carried out with Shimadzu UV-visible spectrophotometer (model 1650 PC) and Shimadzu spectrofluorimeter (model RF-5301) respectively. Fluorescence lifetime measurements were performed using a pico-second laser and a single-photon counting setup from Jobin-Yvon IBH (Madras University, Chennai, India). The fluorescence decay of the sample was analyzed using IBH data analysis software. FTIR spectra of the drugs, CDs and the inclusion complexes were measured from 4000 cm^{-1} to 400 cm^{-1} on a JASCO FTIR-5300 spectrometer using KBr pellet with 256 scans at a resolution of 4 cm^{-1}. One-dimensional ^{1}H NMR spectra for the drugs and its CD inclusion complexes were recorded on a Bruker AVANCE 500 MHz spectrometer (Germany) using an inverse broadband (BBI) probe at room temperature. Samples were dissolved in DMSO-d_6 (99.98%) and were equilibrated for at least 1 hr. Thermal characteristics of solid inclusion complexes were measured using Mettler

Toledo DSC1 fitted with STR^e software (Mettler Toledo, Switzerland), temperature scanning range was from 25 to 180 °C with a heating rate of 10 °C/min. Microscopic morphological structures of the solid samples as well as LC, PC, α-CD and β-CD were investigated and photographed using a scanning electron microscope Hitachi S3400N. The morphological structures of drug-encapsulated complexes LC:CD and PC:CD were investigated by TEM using TECNAI G^4 microscope with an accelerating voltage of 200 kV, for the TEM analysis carbon coated copper TEM grids (200 mesh) were used. XRD patterns of powder samples were recorded with a BRUKER D8 Advance diffractometer (Bruker AXS GmbH, Karlsruhe, Germany) with Cu KαI radiation (λ = 1.5406 Å), a voltage of 40 kV and a 20 mA current.

2.5. ^{1}H NMR spectral values for LC and PC

In general, the chemical shift values of the guest protons tend to exhibit appreciable changes when the guest molecule included into the CD cavity. ^{1}H NMR spectra display the effect of CDs on the chemical shifts of drug protons at 25 ºC. The chemical shifts observed for LC, PC and its inclusion complexes (in parenthesis) are as follows:

LC: H_a = 9.174 (9.151/9.143), H_b = 7.067 (7.051/7.045), H_c = 3.136 (3.168/3.176), H_d = 2.619 (2.363/2.639), H_e = 2.133 (2.089/2.079), and H_f = 1.072 (1.079/1.080); and PC: H_a = 10.317 (10.283/10.269), H_b = 9.587 (9.554/9.528), H_c = 9.008 (8.998/8.994), H_d = 7.365 (7.354/7.350), H_e = 7.253 (7.243/7.264), H_f = 7.187 (7.171/7.176), H_g = 2.230 (2.258/2.279), H_i = 2.848 (2.850/2.854), H_j = 1.678 (1.677/1.679), H_k = 1.563 (1.561/1.560), and H_l = 0.922 (0.924/0.923).

2.6. Molecular modeling

Molecular modeling of the inclusion complexes were carried out using Gaussian 03W program. Considering the large number of atoms in the studied systems, an adequate choice of the modern chemistry had to inevitably result from a compromise between the available computer power and the desired level of calculation. The compromise was particularly important

for full geometry optimization calculations, since these tasks were computationally expensive at the *ab initio* level for such large system. Because the semiempirical PM3 method has been shown to be a powerful tool in the conformational study of CD complexes and has high computational efficiency in the calculating CD system, it was selected to study the inclusion process. The initial geometries of LC, PC, α-CD and β-CD were constructed, with Spartan 08 and then optimized by PM3 method. The glycosidic oxygen atoms of CDs were placed onto the XY plane and their centre was defined as the centre of the coordination system. The side chain of the guest molecule was initially placed on to the Z-axis. The positions of the LC and PC molecules were determined by Z-coordinate. We optimized both A (aromatic ring inserted into the cavity) and B (aliphatic chain inserted into the cavity) orientation.

3. Results and discussion

3.1. UV-visible spectral studies

UV-visible spectroscopy is a frequently used analytical technique of choice for investigating the CD inclusion complexation, because of their ability to offer detailed information about the changes in electronic properties of the guests in different media [11-22]. Further, it is well known that different native CDs have the ability to form different inclusion complexes, whose stability constants can be determined by different methods [8]. In aqueous solution, tthree absorption maxima were appear at 271, 261 and 223 nm for LC and 270 and 225 nm for PC (Fig S1). With an increasing the CD concentrations, the relative absorbance of both drugs are increased at the same wavelength. In both CD solutions, the increase in absorbance suggests that both drugs (LC and PC) encapsulated in the hydrophobic CD nanocavities. In addition, a clear isosbestic point (at 230 nm and 220 nm for LC and PC respectively) is observed in the absorption spectra indicating that the existence of 1:1 inclusion equilibrium between the drug and CD molecules [11-22].

3.2. Fluorescence spectral studies

The changes in fluorescence emission spectra of CD encapsulated drugs can be employed to investigate the inclusion complexation process in more detail [23, 24]. The effects of increasing concentration of α-CD and β-CD on the emission spectrum of LC and PC in aqueous solution are illustrated in Fig. 2. The excitation wavelength was fixed at 270 nm for both drugs. In aqueous solution (pH ~ 6.5) both drugs exhibit two emission bands when excited at temperature. Among the two bands, one occurs in shorter wavelength region (SW, ~ 310 nm) along with shoulder at 330-340 nm and the second appears in the longer wavelength region (LW ~ 435 nm). The LW is red shifted from water to CD solutions and the fluorescence intensity of the LW band increases with increase in the $\lambda_{excitation}$ ~ 260 nm to 290 nm (Fig 3). Compared to α-CD, both LW and SW intensities are largely enhanced in the β-CD solutions.

The normal fluorescence takes place from the locally excited (LE) state, while the *twisted intramolecular charge transfer* (TICT) is responsible for highly Stokes shifted fluorescence. In our earlier publications, the reason for the formation of TICT band was explained in detail [14-22]. These effects are usually brought about by the influence of the typical properties of the amide (O=C–N–H) group [14-22]. Due to the resonance existing in the ground state, the C–N bond in the amide group has partially a double bond character. However, the optimized structures by semiempirical quantum mechanical (PM3) calculations showed same preferential ground state configurations for the drug molecules and SW emission suggested a similar configuration of the locally excited state to that of the ground state. The fluorescence results have also suggested that twisted conformation of electron donor (–NH) group with respect to electron acceptor (C=O) group in polar environment is responsible for highly Stokes shifted charge transfer fluorescence for both drugs. As can be seen in Fig. 2 and Fig 3 upon the addition of CD, the fluorescence intensities of the drug molecules are considerably intensified. However, LW (440 nm) emission band is red shifted with increasing the concentrations of CD and both SW and

MW emission band merged in the β-CD solutions (in the region at ~ 322 nm). These data revealed that stable inclusion complexes were formed between the above drug molecules and CD nanocavity. It is interesting to note that, the emission maxima and spectral shape of LC and PC drugs is similar at higher CD concentrations indicates that similar types of inclusion complexes are formed. The CD cavity provided a less polar environment for drug molecules and thus increased the quantum yield of the fluorescence of drugs.

The binding constant and stoichiometry for inclusion complex formation has been determined by the changes in the absorbance and fluorescence intensities with the CD concentrations. The binding constant (K) values are determined by using Benesi-Hildebrand relation [25] indicates that 1:1 complexes are formed between drugs and CD. In the present cases, 1:1 complexes formed between the CD and both drugs were determined using the following Eq.:

$$\frac{1}{I - I_0} = \frac{1}{I' - I_0} + \frac{1}{K\,(I'-I_0)\,[CD]_0}$$

where $[CD]_0$ represents the initial concentration of α-CD and β-CD, I_0 and I are the absorbance and fluorescence intensities in the absence and presence of CD respectively and I′ is the limiting intensity of absorbance and fluorescence. The '*K*' values were obtained from the slope and the intercept of the plots (Fig. 4). Benesi-Hildebrand [25] plot of $1/I - I_0$ against 1/[CD] should yield a straight line (Fig. 4). The plot of $1/I - I_0$ versus 1/[CD] for the inclusion complexation of both LC and PC showed a linear relationship. This analysis reflects the formation of 1:1 inclusion complex between the drugs and CDs. The binding constant (*K*) for the inclusion complexation obtained from the slope and intercept of the plots was found to be LC/α-CD ≈ abs ~193, flu ~ 429, LC/β-CD ≈ abs ~ 316, flu ~715, PC/α-CD ≈ abs ~ 203, flu ~ 259 and PC/β-CD ≈ abs ~ 384,

flu ~ 577 M^{-1}. The variation in the binding constants suggested that the inclusion capability of CDs with drug molecule. In other words β-CD has greater inclusion ability than α-CD.

The thermodynamic parameter, free energy change values (ΔG, in kcal mol^{-1}) for the binding of drug molecules within the α-CD (abs ~ -3.16, flu ~ -3.64 for LC and abs ~ -3.19, flu ~ -3.34 for PC) and β-CD (abs ~ -3.46, flu ~ -3.98 for LC and abs ~ -3.58, flu ~ -3.82 for PC) were measured. The negative ΔG values of the complexes suggest that the binding process is spontaneous and thermodynamically favored in the experimental temperature range (303 K).

3.3. Time-resolved fluorescence studies

In order to further characterize the inclusion complexation process, the time resolved fluorescence study was performed. The time-resolved fluorescence decays of LC and PC in water, α-CD and β-CD (10×10^{-3} mol dm^{-3}) were measured by exciting at 295 nm and using the emission wavelength at 305 nm. The fluorescence decay analysis demonstrating that the lifetime of drugs in aqueous solution was significantly affected by the addition of CD concentration. The fluorescence decays of LC and PC in water are fitted with a biexponential decay reveals that two excited state species are present in the drug molecules i.e., locally excited state (LE) species and TICT species. The fluorescence lifetime values indicate that the shorter lived species (LE) with major contribution and the longer lived species (TICT) with minor contribution in the system. The fluorescence decays of drugs in water are independent of the emission wavelength with average lifetime ($<\tau>$) values of 0.55 ns for LC and 1.05 ns for PC respectively. In the presence of CD with drugs, significant difference is observed in the fluorescence decay. In CD solutions, the emission decay of the drugs is fitted to a triexponential function with three lifetime values (τ_1, τ_2 and τ_3). The average lifetime values obtained as follows: LC ≈ 1.42 ns (α-CD), 2.86 ns (β-CD) and PC ≈ 2.09 ns (α-CD), 3.17 ns (β-CD). The fluorescence decay of LC in CD displayed the third long lived component i.e., complexed form of drug is observed in water. Further, the

amplitude of the complexed form in β-CD is larger than that of α-CD confirms the formation of the inclusion complex with β-CD in a higher degree of magnitude. Similar decay features were also observed for PC drug in different media. The above results indicate that when the drug entrapped in the CD nanocavity, it undergoes a conformation motion in ns-time scale followed by a fast TICT reaction [26].

3.4. FTIR spectral studies

FTIR spectroscopy is a preliminary analytical tool for confirming the formation of the inclusion complexes. Generally in the inclusion complex, the non-covalent interactions such as hydrophobic interactions, van der Waals interactions and hydrogen bondings between the guest and host molecules lead the lower energy of the included part of guest and reduce the peak intensities of the corresponding frequencies [27, 28]. Fig. S2 depicts the FTIR spectra of LC, PC and the inclusion complexes (LC: α-CD, LC: β-CD, PC: α-CD and PC: β-CD) within the wave number range from 4000 to 400 cm^{-1}. The characteristic bands of LC are found at 3252 cm^{-1} for N–H symmetric stretching, 1665 cm^{-1} for C=O stretching, 1497 and 1593cm^{-1} for C=C stretching vibration in aromatic ring, 2969 and 2865 cm^{-1} for CH stretching vibration, 2972 cm^{-1} for C–H stretching in $–CH_2$ group and 492 cm^{-1} for C–N–C bending vibration. The weak bands in the region 2000 - 1700 cm^{-1} are due to the overtones and combinations of the phenyl ring. The five bands located at 1035, 1074, 1106, 1166 and 1208 cm^{-1} are attributed to CH in-plane bending and a sharp band for CH out-of-plane bending vibrations for aromatic ring was obtained at 765 cm^{-1}. However, the FTIR spectrum of each inclusion complexes showed some significant differences when compared to pure LC spectrum. The bands at 1497 and 1593 cm^{-1} corresponding to the aromatic C=C stretching vibrations disappeared in the inclusion complexes (Fig. S2 b and c). The bands due to overtones, combination vibrations and CH in-plane bending vibrations of aromatic ring are also completely disappeared. This is because the phenyl ring of the drug entrapped into the CD cavity as a result of inclusion complex formation.

FTIR spectra for the isolated PC (Fig. S2 d) showed its characteristics bands in agreement with the previously reported literature [29]. As like in LC, there are apparent differences observed between the PC and the inclusion complexes (Fig. S2 d, e and f). For example, the C=O stretching appears at 1706 cm^{-1} shifted to 1637 cm^{-1} in the inclusion complex. The N–H stretching vibrations appear at 3206 and 3402 cm^{-1} were completely disappeared in the inclusion complexes. In addition, both the amidic N–H bending vibration (1539 cm^{-1}) and C–N–C bending vibration (498 cm^{-1}) frequencies were disappeared. The CH in-plane bending vibration at 1042 and 1112 cm^{-1} are disappeared and the intense band at 761 cm^{-1} (due to CH out-of-plane bending vibration) is shifted in the inclusion complexes. The above results confirmed that the inclusion complex was formed between the PC and the CDs and the benzene ring of PC was encapsulated into the CD cavity. From FTIR results, it was inferred that the presence of CH stretching of methylene ($–CH_2$) group of the drugs with comparable weak shift in the inclusion complexes indicates the aliphatic chain was not involved in the inclusion complex formation.

3.5. Differential scanning colorimetry (DSC)

The thermal properties of the inclusion complexes were investigated by differential scanning colorimetry (DSC). Generally, when the guest molecules encapsulated into CD nanocavities, their melting and sublimation points shift to different temperature or disappeared. The thermal curves of LC, PC and the corresponding inclusion complexes are shown in Fig. 5. The thermal curve of LC exhibited a sharp endothermic peak at 67.8 ºC, corresponding to the melting point of the drug. Whereas in PC, the initial flatted profile and followed by a sharp endothermic peak at higher temperature (167.6 ºC) was obtained. The sharp melting peaks are an indicative of the crystalline anhydrous nature of the drugs. The DSC profile of α-CD showed three endothermic peaks around at ~79, 109, 137 °C and a broad endothermic peak at ~128 °C was observed for β-CD. These endothermic effects are mostly associated to crystal water losses i.e., dehydration process from the CD cavities. The DSC analysis revealed that the melting point for the drug

molecules completely changed or disappeared in the inclusion complex. The shift of dehydration peaks of CDs to lower temperature and compared to pure CDs, the reduction of the relative peak intensity indicated that the dehydration process occurs faster at lower temperature in the inclusion complexes. The DSC data clearly suggesting that both drugs (LC and PC) are deeply encapsulated in the CD nanocavity.

3.6. ^{1}H NMR spectral studies

^{1}H NMR spectra of LC, PC and the inclusion complexes were recorded to obtain deeper insight into the interaction of the drugs with CDs (Fig S3 and S4). The chemical shifts of CD protons reported by different authors [30] are very close to those reported in this work. H-3 and H-5 protons are placed in the interior hydrophobic part of the CD cavity and the interaction of the guest (LC and PC) with the inside CD cavity affects the chemical shifts of the H-3 and H-5 protons (Fig. S3 and S4). A minor shift is observed for the H-1and H-6 protons are located on the edge of the CD cavity, these protons are involved in intermolecular hydrogen bond with the guest. The resonance patterns of LC, PC and the inclusion complexes were slightly different from corresponding uncomplexed molecules (see section 2.5).

In the ^{1}H NMR spectra, the protons of PC and LC (H_a and H_b) and the inner CD cavity protons (H-3 and H-5) are different and can be used to monitor the interaction between the drugs and CDs. The resonance assignment of CD protons are well established [31] and consists of six types of protons, the chemical shift of CD protons reported by different authors are very much closer to those reported in this work. It is evident that the presence of drug produced upfield shift of all signals in CD protons. However, important chemical shifts changes were observed in the inner protons (H-3 and H-5) of the CD. In contrast, no considerable changes were observed for protons located outside of the CD cavity (i.e., H-1, H-2 and H-4). The upfield shift of H-3 and H-5 protons was also significantly larger in comparison to that of the H-6 proton which is located

on the primary face. Further the larger shift of the H-3 proton in comparison with H-5 indicates that the drug molecules entered into the CD cavity from its wider rim side.

Compared with the corresponding free drug molecule, the chemical shifts of phenyl protons (H_a and H_b) and methyl protons (H_c and H_e) of LC drug is shifted downfield upto 0.023 ppm in LC/α-CD complex and 0.054 ppm in LC:β-CD complex. Further, in PC, the chemical shift values of H_a, H_b, H_c, H_d, H_e and H_f protons exhibited significant changes (0.011-0.059 ppm). These results indicated that the phenyl part of LC or PC molecules strongly interacts with the CD cavities and the drugs have inserted into the CD cavity from the wider rim side. On the contrary, the aliphatic protons of LC (H_d and H_f) as well as PC (H_i, H_j, H_k and H_l) were only slightly affected after the complexation with CDs, indicating that both drugs protons did not enter into the hydrophobic cavity of CD. However, the chemical shift changes in drug: β-CD complex is greater than those of drug: α-CD complex indicates the drugs deeply encapsulated in the β-CD cavity.

3.7. XRD analysis

The formation of inclusion complexes can be further confirmed by x-ray diffractometry (XRD). The powder XRD patterns of LC, PC and the inclusion complexes are presented in Fig. 6. The diffractogram of LC exhibited a series of sharp and intense peaks at diffraction angles (2θ) of 8.01, 9.18, 10.19, 12.55, 13.65, 14.92, 19.84 and 24.94º, indicating the crystalline nature of the drug. Similarly in PC, the crystalline nature is confirmed by the sharp peaks at 2θ values of 7.01, 13.01, 14.74, 16.74, 18.75, 19.57, 21.57, 22.84, 24.57, 25.67, and 27.12º. The diffraction patterns obtained for both α-CD and β-CD also showed that both CDs are crystalline substances. This is because the presence of characteristic peaks at diffraction angles (2θ) of 9.46, 11.82, 14.19, 17.93, 21.57, 27.12º and 8.95, 10.56, 12.46, 18.75, 22.57, 27.03, 31.86, 34.59º respectively. On contrary, the XRD spectrum of the inclusion complexes showed considerable diversity when comparing with the pure drugs as well as CD (Fig. 6). The diffractogram of the

inclusion complex was found to be disappear of characteristic peaks at (2θ) 8.01, 10.19, 15.01º for LC and 7.01, 14.74, 24.57, 34.94º for PC indicating loss of their crystalline nature [32]. In addition, the sharpness of peaks as well as the number of sharp peaks existing with pure drug was found to be significantly diminished in the case of complex which may probably be due to the existence of drug in a totally different form other than crystalline as a result of processing during the formation of inclusion complex.

3.8. Scanning electron microscopy (SEM)

SEM analysis reflected that the drug-CD inclusion systems led to a drastic change in shape and size with respect to the original components. Selected micrographs of LC, PC and their inclusion complexes are illustrated in Fig.7. Pure LC in powder form appeared as lamellar crystals, while pure PC looked like plate shaped crystals. α-CD particles showed prismatic crystals with well-developed faces whereas β-CD particles consisted of large crystals with a parallelogram shape. The original morphology of both drugs and CDs are disappeared in the inclusion complexes and amorphous halo aggregates with irregular shape were observed and it was no longer possible to distinguish the initial components, as shown in the inclusion complexes in Figs. 7d, e, g and h.

3.9. Transmission electron microscopy (TEM)

The morphological characteristics of inclusion complexes were further examined by using TEM and the results are shown in Fig. 8. TEM micrographs have been utilized to measure the length as well as to find out the shape of supramolecular self-assembly. To visualize via TEM, the samples were prepared from two drops of the solution of the drug: CD was kept onto carbon-coated copper grid without any further coating. Interestingly, in the presence of water, spherical nanoparticles were observed in all the case of assemblies (Fig.8). The particles were morphologically homogeneous in each assembly. It could be found that the diameter size of PC:

β-CD particles (~ 200 nm) are slightly larger than those of other assemblies (~ 60 - 80 nm). In addition, in the aqueous solutions of the CD or drug, no such well-defined nano aggregates were detected by TEM. Thus, the combination of drug and CD is significant for the formation of particles in nanoscale. In fact, the absorption and fluorescence data indicated that CD can encapsulate the drugs in a 1:1 molar ratio, which is similar to the analogous inclusion complexes previously reported by other researchers [33, 34].

3.10. Molecular modeling study

In order to rationalize the experimental results as described above and to further understand the mechanism of the inclusion complexation of the LC and PC drugs with α-CD and β-CD, we performed theoretical calculations using semiempirical quantum mechanics at PM3 level of theory [35]. In this study, two possible orientations were considered: (i) the aromatic ring oriented to the centre of CD cavity, namely orientation-A and (ii) the aliphatic chain oriented to the centre of CD cavity, namely orientation-B (Fig. S5). The values used in the calculation of these magnitudes are the ones obtained in the frequency analysis carried out with the PM3 method. This analysis was performed on the structures of the complex with the lowest energy which were obtained during the simulation of the inclusion process in each one of the orientations considered.

For the inclusion complexes of the above drugs in both orientations, it was observed that the drug approaches the CD cavity from its secondary face and the binding energy decreases gradually until a minimum is obtained. As the drug molecule is inserted into the CD cavity it rotates to adjust itself in a position to maximize the interactions with the inside of the cavity and to minimize steric hindrance caused by the methyl group. A minimum energy is obtained when the phenyl group of LC or PC is completely inserted into the cavity while the carbonyl group of the drug molecule is attached to the CD protons via strong hydrogen bonding. The structures of

the complexes obtained with the lowest energies were subsequently optimized without any constraints (Fig. S5).

The complexation energies of the drug molecules with α-CD and β-CD (for orientation-A) obtained from the PM3 calculations are given in Table 1. The results showed that the complexation energies (in kcal mol^{-1}) of all the complexes (LC: α-CD ≈ orientation-A = -1295.46, orientation -B = -1283.52; LC: β-CD ≈ orientation -A = -1514.84, orientation -B = -1499.84; PC: α-CD ≈ orientation -A = -1310.10, orientation -B = -1298.13; PC: β-CD ≈ orientation -A = -1531.82, orientation-B = -1522.17) are negative which demonstrates the inclusion processes are thermodynamically favour for both orientations (A and B). Further, more negative complexation energy is obtained in the stable inclusion complex and the more favourable is the configuration. It was found that the complexation energy for orientation-A in each step was always lower than that of orientation-B. These results revealed that the complexation energy is in more favourable for the orientation-A with significant energy gap and the nature of the driving forces leading to the favourable orientation. Hence, the most stable structures were gathered from the energies of the complexes for probable orientations in which the phenyl ring located within the CD cavity (Fig. S5).

To investigate the thermodynamics of the binding process, the binding energy (ΔE), enthalpy change (ΔH), Gibbs free energy change (ΔG) and entropy change (ΔS), of the guests and hosts were carried out by the PM3 method for orientation-A at 1 atm pressure and 298.15 K temperature. The thermodynamic parameters are summarized in Table 1. Further, we have determined the binding energy (ΔE) in order to quantify the interaction between drugs with α-CD and β-CD in the optimized geometries. Once again the large negative binding energy (ΔE) for the formation of complexes in orientation-A revealed that the CDs could form stable complexes with drugs. However, the difference of binding energies for the inclusion complexes of the drugs

with CDs is 9.25 kcal mol^{-1} (for LC) and 11.59 kcal mol^{-1} (for PC) respectively, suggests that the drug/β-CD complex is more stable than that of α-CD complex.

Among both A and B orientations, the phenyl ring inserted orientation was more energetically favored for drug: CD complexes. Therefore, here we discuss the thermodynamic results for only orientation-A. From Table 1 it can be seen that: (i) in both LC and PC, the binding energies of the β-CD complexes are about ~10.0 kcal mol^{-1} lower than that of the complexes formed by α-CD. The above results suggested that the β-CD formed more stable inclusion complexes with LC and PC drugs, (ii) binding energies for PC: CD inclusion complexes are lower (~15 kcal mol^{-1}) in comparison to that of the LC: CD complexes, (iii) the negative ΔH and ΔS values indicated that the formation of all the four inclusion complexes is an enthalpy driven processes and (iv) the positive free energy changes (ΔG) of the inclusion complexes implied that inclusion proceeded non-spontaneously under the experimental conditions.

The experimental ΔG values are negative whereas theoretical ΔG values are positive. The difference in Δ*G* can be explained by the solvent effect. The experiments were conducted in aqueous medium and the computational work was done in vacuum phase [36-39]. We were unable to do the computational work at the aqueous medium due to system limitations. Unfortunately because of limitations in the calculation ability of the computer and the large molecular size of the CD, calculations for these systems could not be performed for aqueous solutions and excited state. However, it is observed that the solvent effect on the host-guest interactions easily changes the inclusion reaction from a non-spontaneous process in the gas phase to a spontaneous one in the aqueous phase. The host-guest interaction causes an enthalpy-entropy compensating process in the gas phase whereas the same interaction causes an enthalpy-entropy co-driven process in aqueous solution, due to release of number of water molecules from the cavity of β-CD in inclusion complexation.

The geometrical parameters, bond distances, bond angles and the most interesting dihedral angles of LC and PC molecules before and after inclusion complex formation for the most stable structures in orientation-A is also determined. The geometrical structures of both drugs after complex formation were completely altered. This alteration was significant in the dihedral angles, which indicated that the drugs adopted a specific conformation to form a stable inclusion complex. This justified the importance of conformational changes of both drugs to ensure a better inclusion of the guest into the CDs cavity. Additionally, the conformation of both CD was also significantly altered during complex formation. We found that the round cavity of CD turned into an oval shaped cavity (Fig. S5). Further the changes in the geometrical parameters were supported by the fact that the flexibility of the host molecules may be one of the structural requirements upon the inclusion complex formation. The overall PM3 calculation results are in good agreement with that of the experimental results.

4. Conclusion

The following conclusions can be drawn from the above studies: (i) both LC and PC drugs form 1:1 inclusion complex with α-CD and β-CD, (ii) triexponential decay in CD solution indicated that the drug molecules undergo effective microencapsulation, (iii) TEM examinations demonstrated that the self-aggregates of drug: CD are nano sized particles and the nanoparticles are stable and spherical in shape with a narrow size distribution, (iv) thermodynamic parameter (ΔE, ΔH, ΔG and ΔS) results confirmed the stability of the inclusion complexes and (v) the geometry of the most stable complex showed that the aromatic ring is deeply included into the CD nanocavity and intermolecular hydrogen bonds were established between host and guest molecules. This suggested that hydrophobic effect and hydrogen bonds play a vital role in the inclusion process.

Acknowledgements

This work is supported by the Council of Scientific and Industrial Research [No. 01(2549)/12/EMR-II] and University Grants Commission [No. F-351-98/2011 (SR)], New Delhi, India.

References

[1] J. Szejtli, In Comprehensive Supramolecular Chemistry. Oxford, UK, (1996).

[2] S. Li, W. C. Purdy, Chem. Rev. 92 (1992) 1457–1470.

[3] K.A. Connors, Chem. Rev. 97 (1997) 1325–1358.

[4] H. Schneider, F. Hacket, V. Rudiger, Chem. Rev. 98 (1998) 1755–186.

[5] B. Yang, J. Lin, Y. Chen, Y. Liu, Bioorg. Med. Chem. 17 (2009) 6311–6317

[6] T. Sohajda, S. Beni, E. Varga, R. Ivanyi, A. Racz, L. Szente, B. Noszal, J. Pharm. Biomed. Anal. 50 (2009) 737‑745.

[7] J. Feng, W. Yan, J. Zhu, Syn. Metals 160 (2010) 939–945.

[8] J. Szejtli, Chem. Rev. (1998) 98 1743–1753.

[9] M. Jug, F. Maestrelli, M. Bragagni, P. Mura, J. Pharm. Biomed. Anal. 52 (2010) 9–18.

[10] J. Zeng, Y. Ren, C. Zhou, S. Yu, W-H. Chen, Carbohydr. Polym. 83 (2011) 1101–1105.

[11] G.Krishnamoorthy, S.K.Dogra, J.Photochem. Photobiol. A: Chem. 123 (1999) 109-119.

[12] S.K. Das, Chem. Phys. Lett. 361 (2002) 21-28.

[13] S.Panja, S.Chakravorti, Spectrochim. Acta, A 58 (2002) 113-122.

[14] A.Antony Muthu Prabhu, G.Venkatesh, N.Rajendiran, J. Solution Chem. 39 (2010) 1061-1086.

[15] A.Antony Muthu Prabhu, R.K.Sankaranarayanan, S. Siva, N.Rajendiran, Spectrochim. Acta A, 74 (2009) 484–497.

[16] A.Antony Muthu Prabhu, N.Rajendiran, J.Fluoresc. 22 (2012)1461-1474.

[17] K.Sivakumar, T.Stalin, N.Rajendiran, Spectrochim. Acta A, 62 (2005) 991–999.

[18] A. Anton Smith, R. Manavalan, K. Kannan, N. Rajendiran, J. Fluoresc. 20 (2010) 809–820.

[19] A.Antony Muthu Prabhu, V.K. Subramanian, N. Rajendiran, Spectrochim. Acta A 96 (2012) 95–107.

[20] T.Sivasankar, A.Antony Muthu Prabhu, N.Rajendiran J.Mol. Struc. 1028(2012) 57-67.

[21] A.Antony Muthu Prabhu, R.K. Sankaranarayanan, G. Venkatesh, N. Rajendiran, J. Phys. Chem. B 116 (2012) 9061–9074.

[22] M. Jude Jenita, G. Venkatesh, A.A.M. Prabhu, N. Rajendiran, J. Mol. Liq. 178 (2013) 160–167.

[23] Zhenxing Chi, Rutao Liu, Hao Zhang, Biomacromolecules, 11(2010) 2454-2459.

[24] Wansong Zong, Rutao Liu, Feng Sun,Yue Teng, Xiaoyan Fang, Jun Chai, J. Fluoresc. 21 (2011) 1249-1254.

[25] H.A. Benesi, J.H. Hildebrand, J. Am. Chem. Soc. 71 (1949) 2703–2707.

[26] T.A. Fayed, J.A. Organero, I. Garcia-Ochoa, L. Tormo, A. Douhal, Chem. Phys. Lett. 364 (2002) 108–114.

[27] H.M. Jian, H.J. Sun, S.B. Zhang, R.N. Hua, Y.M. Xu, S.B. Jin, H.Y. Gong, L. Li, J. Incl. Phenom. Macrocycl. Chem. 58 (2007) 133–138.

[28] E.E.M. Eid, A.B. Abdul, F.E.O. Suliman, M.A. Sukari, A. Rasedee, S.S. Fatah, Carbohydr. Polym. 83 (2011) 1707–1714.

[29] J. Wang, Y. Cao, B. Sun, C. Wang, (2011). Food Chem. 127, 1680–1685.

[30] M.V. Rekhasky, Y. Inoue, Chem. Rev. 98 (1998) 1875–1918.

[31] M. Bragagni, F. Maestrelli, P.J. Mura, Incl. Phenom. Macrocycl. Chem. 68(2010) 437–445.

[32] M. Messner, S.V. Kurkov, P. Jansook, T. Loftsson, Int. J. Pharm. 387 (2010) 199–208.

[33] Y. He, P. Fu, X. Shen, H. Gao, Micron 39 (2008) 495–516.

[34] P.R.K. Mohan, G. Sreelakshmi, C.V. Muraleedharan, R. Joseph, Vibrational Spec. 62 (2012) 77–84.

[35] M. Karelson, V.S. Lobanov, R. Katrizky, Chem. Rev. 96 (1996) 1027–1044.

[36] Hamdi H, Abderrahim R & Meganem F, Spectrochimica Acta Part A, 75 (2010) 32.

[37] Xing S K, Zhang C, Ai H Q, Zhao Q, Zhang Q & Sun D Z, J Mol Liquids, 146 (2009) 15.

[38] M.Jude Jenita, AAM Prabhu, N.Rajendiran, Indian J. Chemistry A, 51A (**2012**) 1686-1694.

[39] G.Venkatesh, T.Sivasankar, M.Karthick, N.Rajendiran, J.Inclusion Phenomena and Macrocyclic Chemistry, 77 (**2013**) 309-318.

Figure Captions

Fig. 1 Chemical structure of (a) lidocaine and (b) prilocaine

Fig. 2. Fluorescence spectra of LC and PC in different α-CD and β-CD concentrations (4×10^{-5} mol dm^{-3}): (1) 0, (2) 0.001, (3) 0.002, (4) 0.004, (5) 0.006, (6) 0.008 and (7) 0.010; $\lambda_{Excitation}$ ~ 270 nm.

Fig. 3. Fluorescence intensity *vs.* CD concentration.

Fig. 4. B-H plots for formation of 1:1 complexes of LC and PC with α- and β-CD: (a,b) Plot of $1/A\text{-}A_0$ vs. 1/[CD] and (c,d) Plot of $1/I\text{-}I_0$ vs. 1/[CD].

Fig. 5. DSC thermograms of (a) α-CD, (b) β-CD, (c) LC, (d) LC:α-CD complex, (e) LC;β-CD complex, (f) PC, (g) PC:α-CD complex and (h) PC:β-CD complex.

Fig. 6. Powder XRD patterns of (a) α-CD, (b) β-CD, (c) LC, (d) LC:α-CD complex, (e) LC:β-CD complex, (f) PC, (g) PC:α-CD complex and (h) PC:β-CD complex.

Fig. 7. SEM photographs of (a) α-CD, (b) β-CD, (c) LC, (d) LC:α-CD complex, (e) LC:β-CD complex, (f) PC, (g) PC:α-CD complex and (h) PC:β-CD complex.

Fig.8. TEM photographs of (a) LC: α-CD complex, (b) LC: β-CD complex, (c) PC: α-CD complex and (d) PC: β-CD complex.

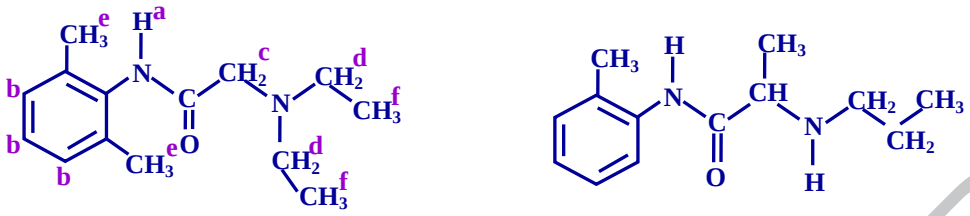

(a) (b)

Fig. 1 Chemical structure of (a) lidocaine and (b) prilocaine

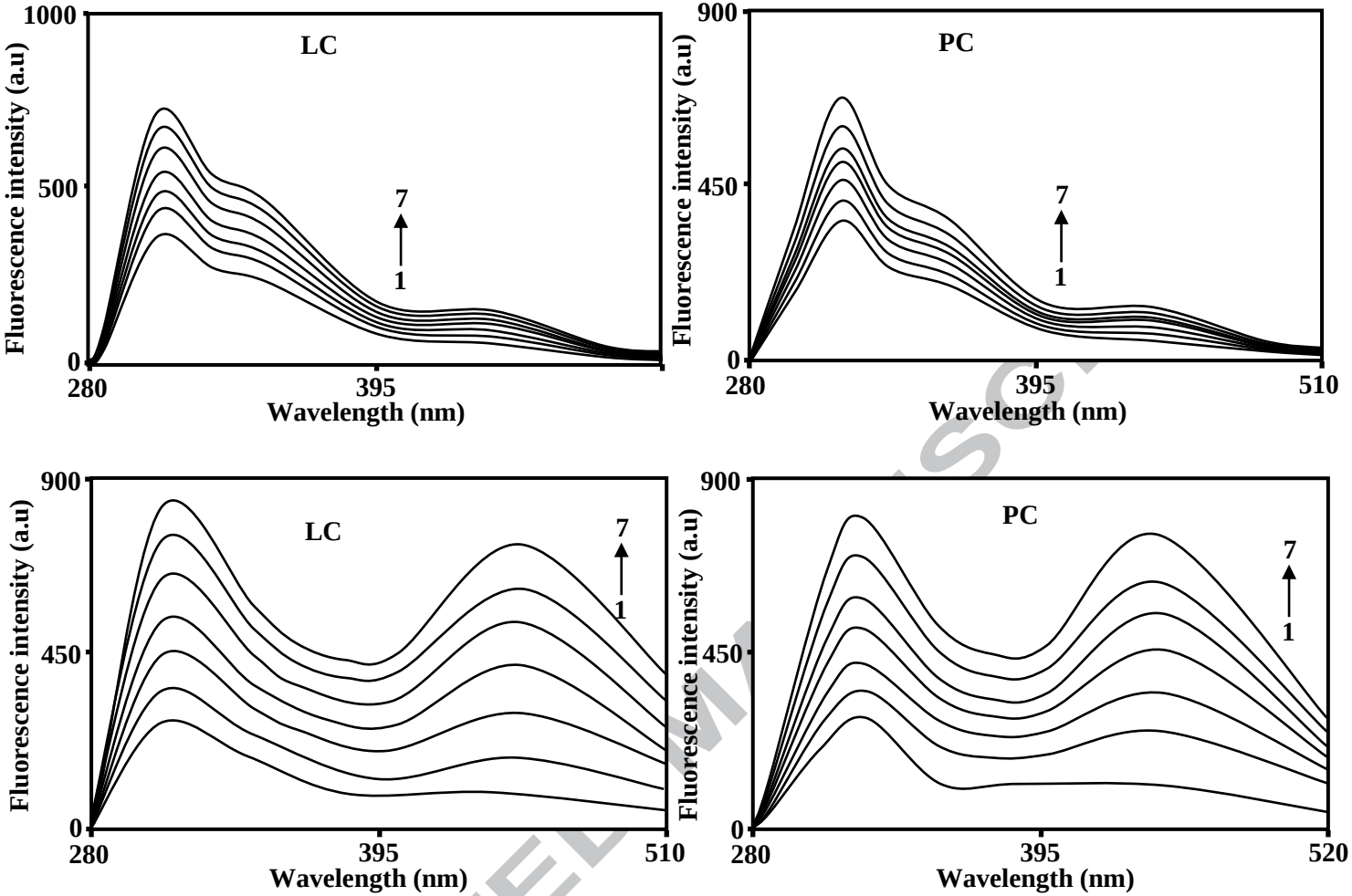

Fig. 2. Fluorescence spectra of LC and PC in different α-CD and β-CD concentrations (4×10^{-5} mol dm^{-3}): (1) 0, (2) 0.001, (3) 0.002, (4) 0.004, (5) 0.006, (6) 0.008 and (7) 0.010. $\lambda_{Excitation}$ ~ 270 nm.

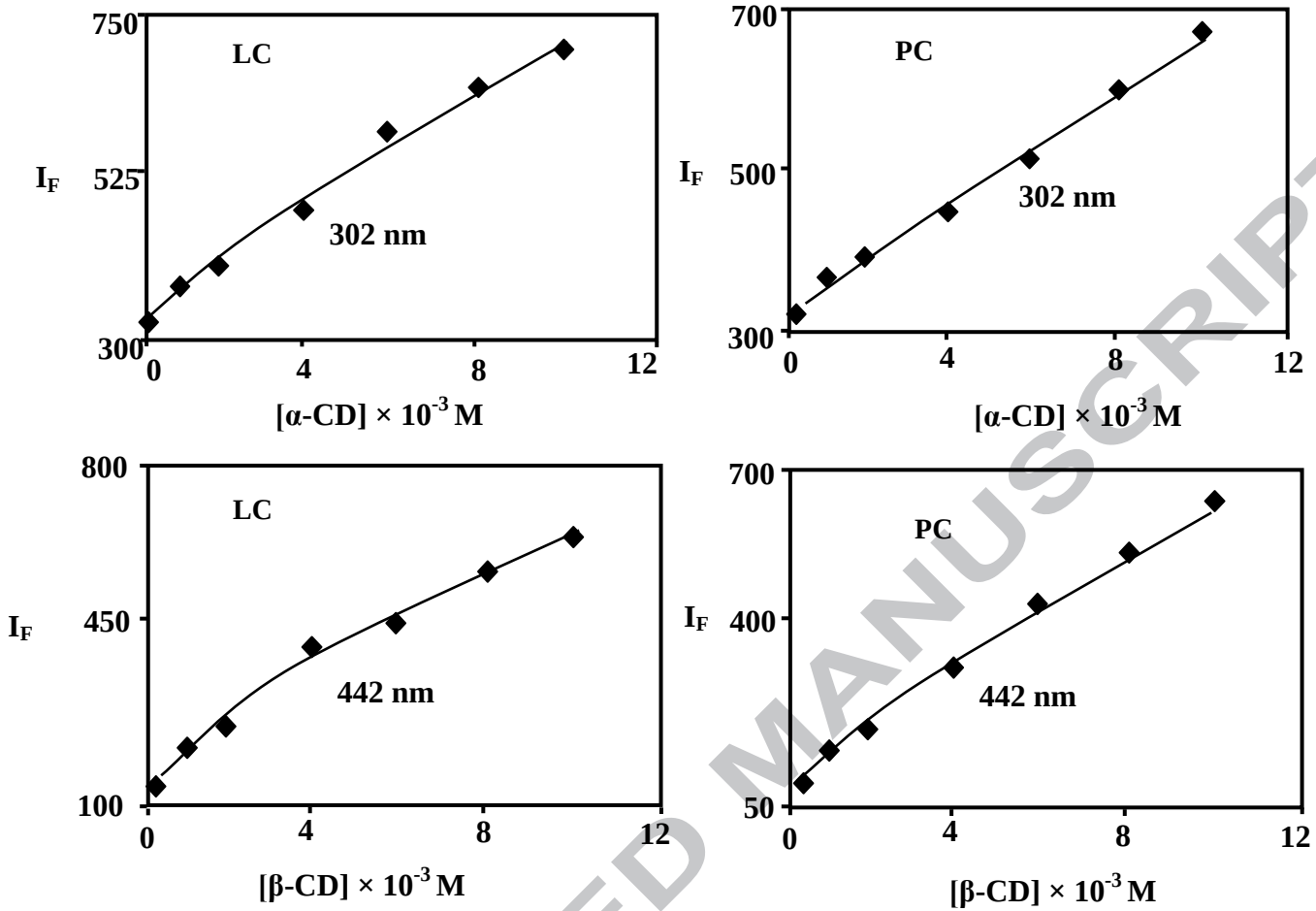

Fig. 3. Fluorescence intensity *vs.* [CD]

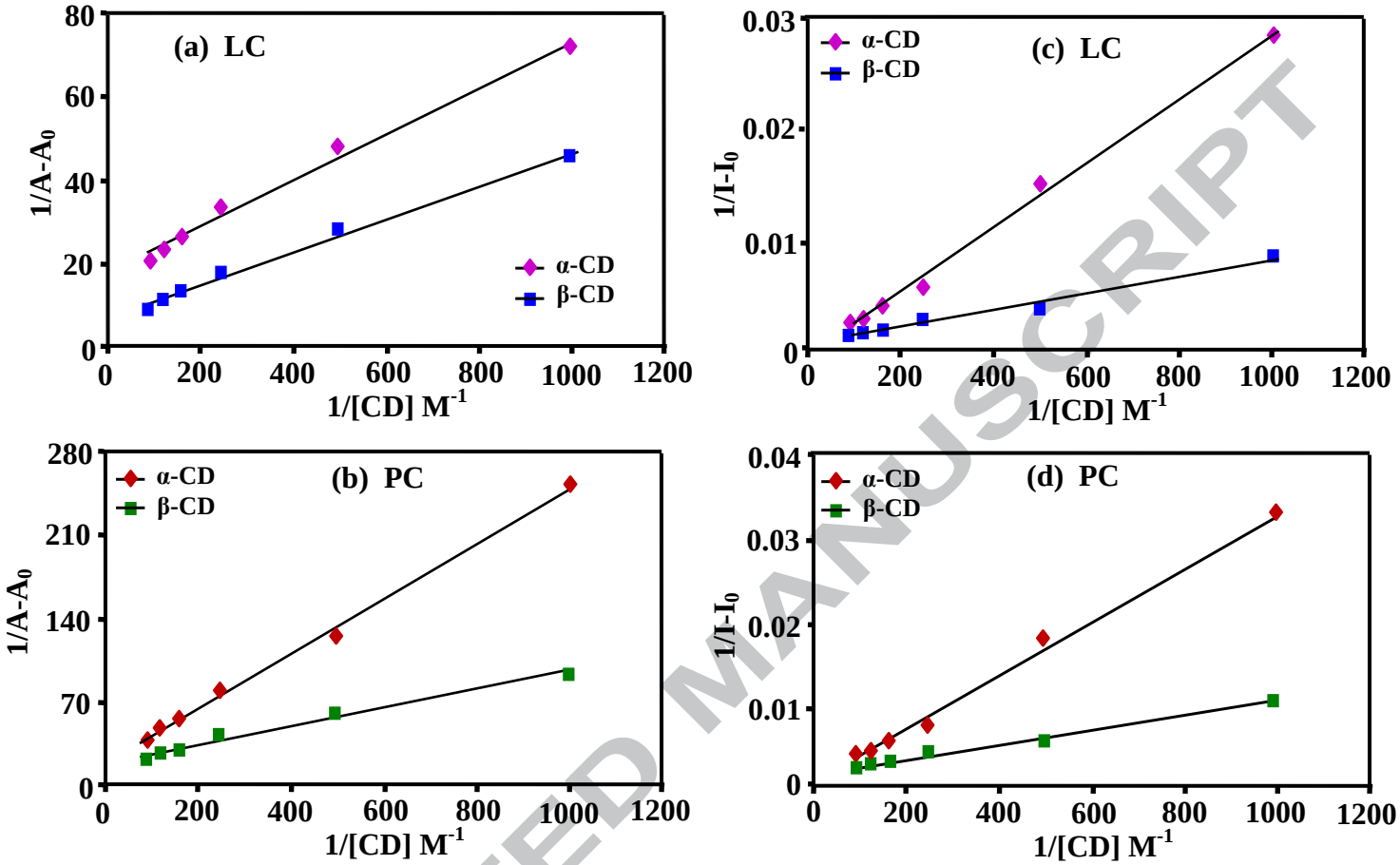

Fig. 4. B-H plots for formation of 1:1 complexes of LC and PC with α- and β-CD: (a,b) Plot of $1/A-A_0$ vs. 1/[CD] and (c,d) Plot of $1/I-I_0$ vs. 1/[CD].

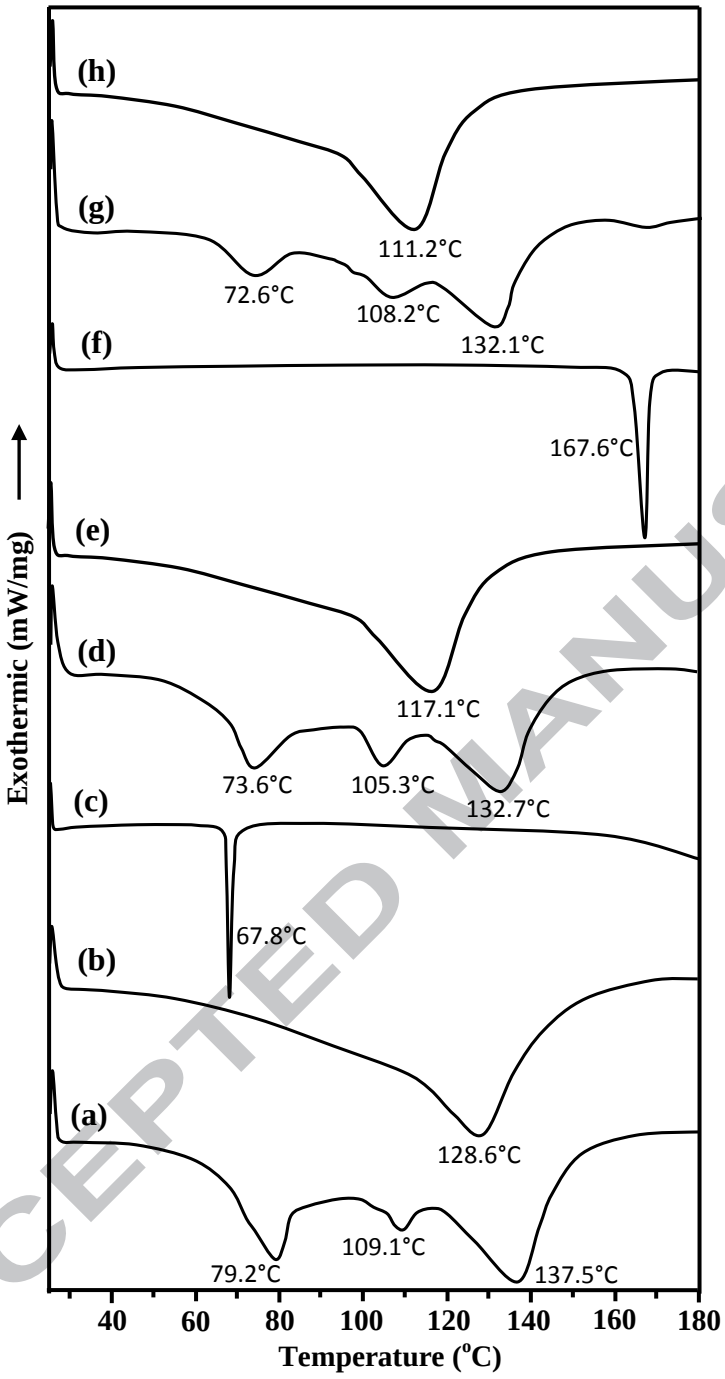

Fig. 5. DSC thermograms of (a) α-CD, (b) β-CD, (c) LC, (d) LC:α-CD complex, (e) LC:β-CD complex, (f) PC, (g) PC:α-CD complex and (h) PC:β-CD complex.

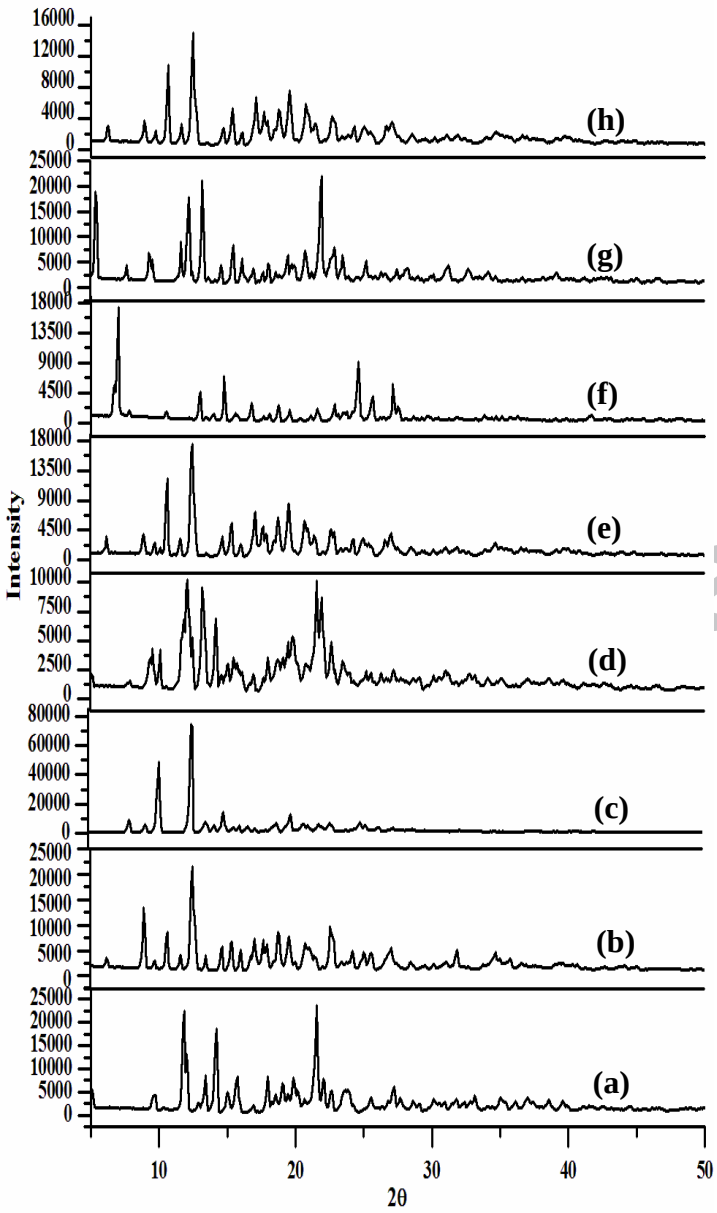

Fig. 6. Powder XRD patterns of (a) α-CD, (b) β-CD, (c) LC, (d) LC;α-CD complex, (e) LC;β-CD complex, (f) PC, (g) PC;α-CD complex and (h) PC:β-CD complex.

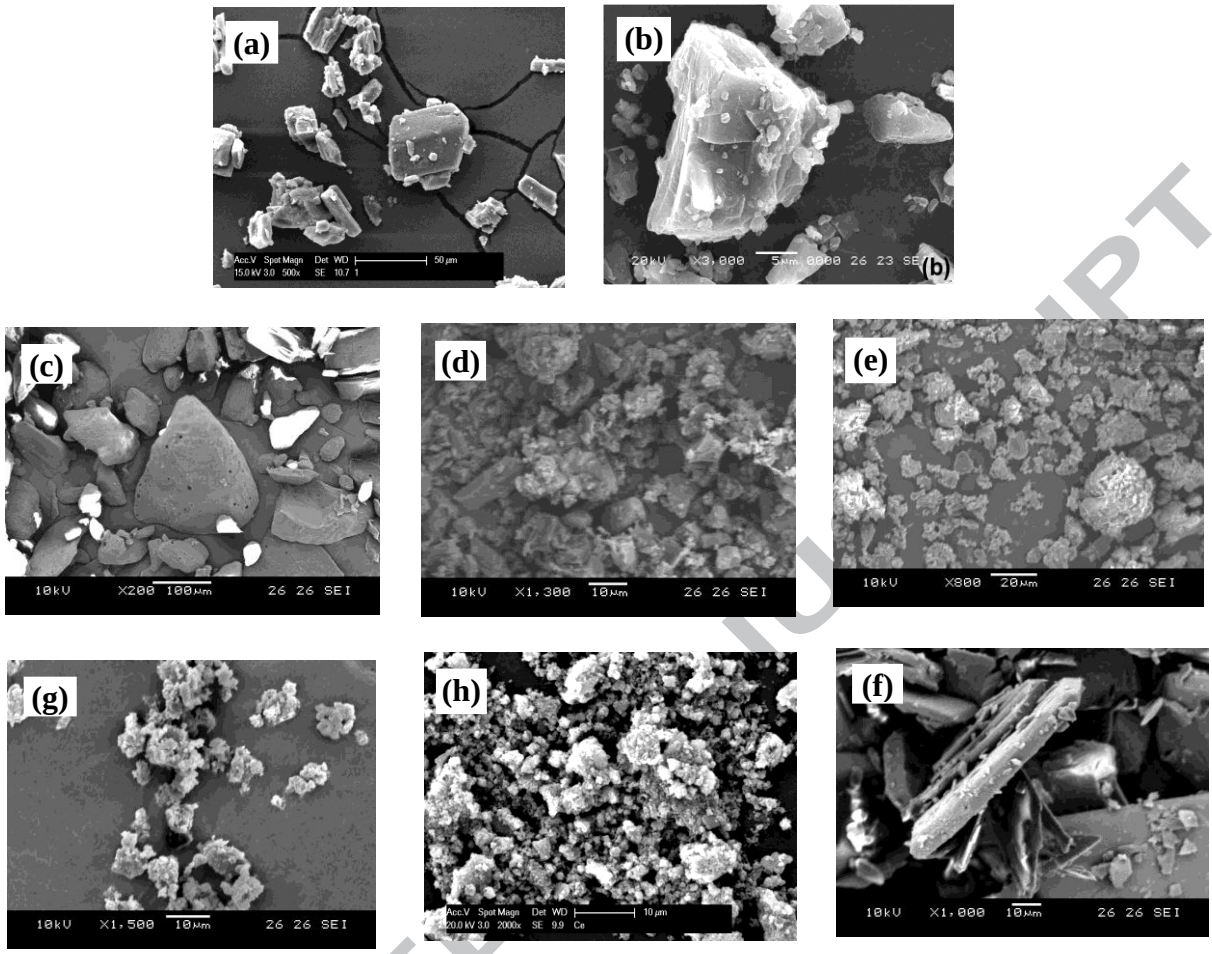

Fig. 7. SEM photographs of (a) α-CD, (b) β-CD, (c) LC, (d) LC:α-CD complex, (e) LC:β-CD complex, (f) PC, (g) PC:α-CD complex and (h) PC:β-CD complex.

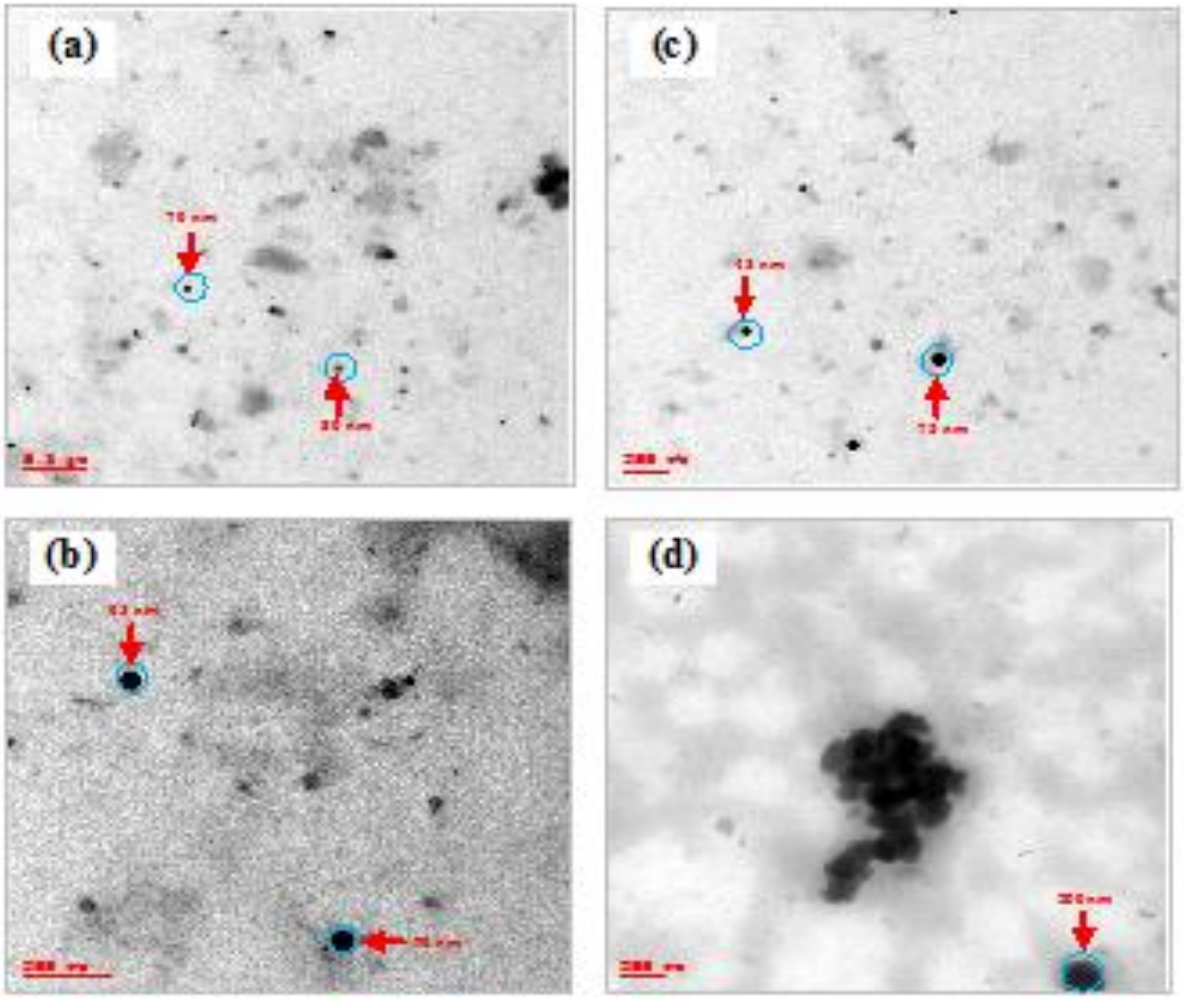

Fig. 8. TEM photographs of (a) LC:α-CD complex, (b) LC:β-CD complex, (c) PC:α-CD complex and (d) PC:β-CD complex.

Table 1
Energetic features and thermodynamic parameters of LC, PC, α-CD, β-CD and its 1:1 inclusion complexes (for orientation-A) obtained by PM3 method

Properties	LC	PC	α-CD	β-CD	LC/α-CD	LC/β-CD	PC/α-CD	PC/β-CD
E (kcal mol^{-1})	-41.87	-52.97	-1247.62	-1457.75	-1295.46	-1514.84	-1310.10	-1531.82
ΔE (kcal mol^{-1})					-5.97	-15.22	-9.51	-21.10
H (kcal mol^{-1})	181.9	159.84	-570.84	-667.55	-396.47	-499.88	-418.72	-526.42
ΔH (kcal mol^{-1})					-6.72	-13.42	-7.72	-18.71
G (kcal mol^{-1})	138.01	118.43	-676.37	-789.52	-504.91	-645.08	-550.41	-669.27
ΔG (kcal mol^{-1})					33.45	6.43	7.53	1.82
S (kcal/mol-Kelvin)	0.144	0.138	0.353	0.409	0.418	0.487	0.441	0.479
ΔS (kcal/mol-Kelvin)					-0.079	-0.066	-0.05	-0.07

Research Highlights

- Both lidocaine and prilocaine drugs form 1:1 inclusion complexes with α-CD and β-CD.
- Spherical size nanoparticles were observed in both drug-CD inclusion complexes
- Aromatic ring is deeply included into the CD nanocavities
- Intermolecular hydrogen bonds were formed between host and guest molecules

Graphical Abstract

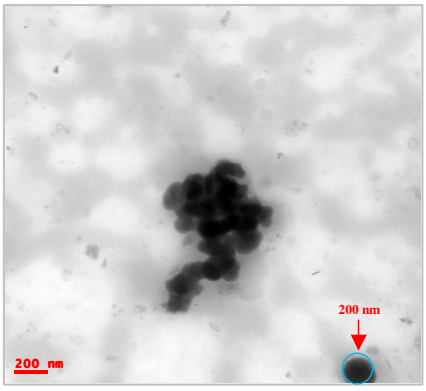

Fig. TEM photographs of PC/β-CD complex.